Journal of Advanced Concrete Technology Vol. 17, 168-176, April 2019 / Copyright © 2019 Japan Concrete Institute

Scientific Paper

Full-Field Settlement Measurement at Fresh Cementitious Material by Digital Image Correlation

Evin Dildar Dzaye[1*], Eleni Tsangouri[2], Geert De Schutter[3] and Dimitrios G. Aggelis[4]

Received 23 January 2019, accepted 12 April 2019 doi:10.3151/jact.17.4.168

Abstract

Monitoring concrete properties at a very fresh state is essential to understand the different ongoing processes. Concrete undergoes strong displacements due to different processes such as, evaporation, water migration, settlement, formation of hydrates, shrinkage, early age cracking. This early state of concrete affects the long-term concrete performance. In the present paper the displacement distribution of fresh cementitious material from plastic state up to hardened state is studied by means of the optical and contactless method of DIC. The principle of DIC realizes a full-field 3D continuous monitoring of the surface displacement. An innovative technique of speckle pattern creation allows monitoring the surface displacement few minutes after casting of cement paste and mortar. The experimental results confirmed the effectiveness and correctness of the new technique giving a global overview much more representative than point measurements with traditional displacement meters.

1. Introduction

After casting, concrete stiffens and hardens with age that leads to concrete volume reduction (Sant *et al*. 2009; Wierig 1990; Wieslaw 2014 and Geike *et al*. 1982). Throughout the hardening process the material shrinks into its casting mould and settles at the free open surface leading eventually to cracks formation (Yamakawa *et al*. 2003).

At early age and as the media is in plastic state, the potential for settlement cracking is high and is attributed to different driving forces: differential settlement (Weyers *et al*. 1982); water evaporation that causes high tensile strength and menisci in the capillary water at the surface (Wittmann 1976; Cohen *et al*. 1990), differential thermal increase due to temperature progress within the fresh concrete (Bertil *et al*. 2002) as well as autogenous shrinkage that appears during the concrete plastic state (Pease *et al*. 2004). Understanding and controlling the plastic state settlement is challenging. Kwak *et al.* (2010) analysed the plastic settlement of mortar based on strain consolidation theory that considers the self-weight and consolidation and compared it with experimental data by means of a noncontact laser measurement device. The distribution of settlement due to self-weight decreases dramatically at approximately 90 min. Combrinck *et al*. (2018) identified the combined effect of plastic settlement and plastic shrinkage cracking of concrete. Plastic settlement cracking presented multiple tensile surface cracks and shear cracks while plastic shrinkage cracking exhibited a single crack pattern throughout the entire depth of the concrete. Lura *et al.* (2006) measured the settlement of mortar containing shrinkage-reducing admixture (SRA) using non-contact laser system. The addition of SRA reduces the settlement resulting in a reduction of plastic shrinkage cracks due to differential settlement.

Plethora of monitoring techniques have been used to track early-age plastic deformation including volume change (Barcelo *et al*. 2011), ultrasonic wave velocity (Carlson *et al.* 2003), electrical conductivity (Topu *et al*. 2012), rheological measurement (Taylor *et al*. 2006) and hydraulic pressure variation (Amziane 2006). These methods cannot provide a full-field settlement measurement. Digital Image Correlation (DIC) appears an effective alternative to those methods. This optical method outperforms other methods since it is continuous, contactless and provides accurate and full-field monitoring of surface strain and cracking. Indicatively, Mauroux *et al*. (2012) and Maruyama *et al*. (2013) applied DIC to study the crack pattern and crack width due to drying in coating mortar and concrete respectively. In an older study, the drying shrinkage cracking was effectively measured using in-plane DIC (Lagier *et al*. 2011).

In previous studies of the authors, settlement distribution has been primarily investigated using DIC (Dzaye *et al*. 2018; Dzaye *et al*. 2019; Dzaye *et al*. 2018). This is a continuation of previous work. This paper focuses on the vertical deformation (settlement) of cement paste and cement mortar in plastic state (few minutes after

[1]Ph.D. student, Department of Mechanics of Materials and Constructions, Vrije Universiteit Brussel, Pleinlaan 2, 1050 Brussels, Belgium.
*Corresponding author, *E-mail:* edzaye@vub.ac.be
[2]Post Dr. Department of Mechanics of Materials and Constructions, Vrije Universiteit Brussel, Pleinlaan 2, 1050 Brussels, Belgium.
[3]Professor, Magnel Laboratory for Concrete Research, Department of Structural Engineering, Ghent University Technologiepark- Zwijnaarde 904, B-9052 Ghent, Belgium
[4]Professor, Department of Mechanics of Materials and Constructions, Vrije Universiteit Brussel, Pleinlaan 2, 1050 Brussels, Belgium.

casting) to study concrete drying process as well as the risk of settlement cracks. The experimental results of DIC will be compared to classical point measurement methods of LVDT. DIC mapping allows evaluating the settlement distribution on the surface that affects the final material properties.

2. Brief overview of DIC principle

Digital image correlation is an optical- numerical, non-contact, full-field surface measurement technique (Lionello *et al*. 2014) that offers the possibility to measure complex displacement and deformation of different materials. A pair of high-resolution cameras builds a stereoscopic vision system to measure the surface deformation. The cameras are synchronized and triggered to simultaneously capture images at a constant time interval. DIC images are analysed in post-processing stage to detect differences at the surface between reference (undeformed) and deformed surface state. Any variation at the image intensity can be associated to deformation at the surface. In this way, the sample surface is covered with randomly distributed white and black speckles. The DIC post-processing software measures the grey intensity of local zones (subsets) (Sutton *et al*. 2009). Displacement in space translated to movement of the speckle pattern is perceived as change on the subset grey intensity degree compared to a reference stage (Lecompte *et al*. 2006).

DIC measurement accuracy depends on the speckle pattern quality controlled by black-white contrast, sharpness and speckles size and distribution. There is no standardized and optimized method to apply the speckles, therefore there is a variety of different application procedures in literature, such as marked pen, spray paint, screen printing and airbrush gun (Barranger *et al*. 2010).

Application of DIC on fresh cement-based materials implies a challenging speckle pattern application since the speckles might move due to bleed water or get absorbed on the wet surface. In this study, the development and effectiveness of a new speckle method is investigated considering black and white thin powder particles distributed in layers on the material surface.

Table 1 Mortar ingredients proportions.

Compounds	Mass [kg]	Volume proportion [%]
CEM I 52.5N	2.62	21.16
Normalized sand	5.24	49.34
water	1.18	29.51

3. Materials and method

3.1 Materials

Standard cement paste was studied with a water -to-cement ratio of 0.4 (by mass). The cement used was type I ordinary Portland CEM I 52.5 N with a Blaine specific surface area of 433 m^2/kg, a density of 3090 kg/m^3 and a chemical composition of CaO 63.9%, SiO_2 20%, Al_2O_3 5.1%, Fe_2O_3 3.4%, MgO 0.8%, Na_2O 0.34%, K_2O 0.75%, SO_3 3.1%, Cl^- 0.05% (by mass). The cement paste was mixed in a laboratory concrete mixer for 3 min at low speed. Following the casting, external vibration was applied by a standard vibration table. Afterwards, the material was poured into a metallic mould of size 150 x 150 x 150 mm (internal dimensions) and was kept at a constant temperature of 20 ± 1°C for 65 h. Besides the cement paste, specimens of cement mortar were similarly prepared using the same cement content, a water -to- cement ratio of 0.45 (by mass) and sand with proportions reported in **Table 1**. Throughout the study, 4 specimens per series were investigated to optimize the speckle pattern as well as its effectiveness. In this paper, the most representative cement mortar and cement paste specimens are presented.

3.2 Experimental method

Above the sample surface a pair of digital cameras (AVT Stingray) were installed, see **Fig. 1(a)**. The resolution of the cameras are 2504 by 2056 pixels. The lens

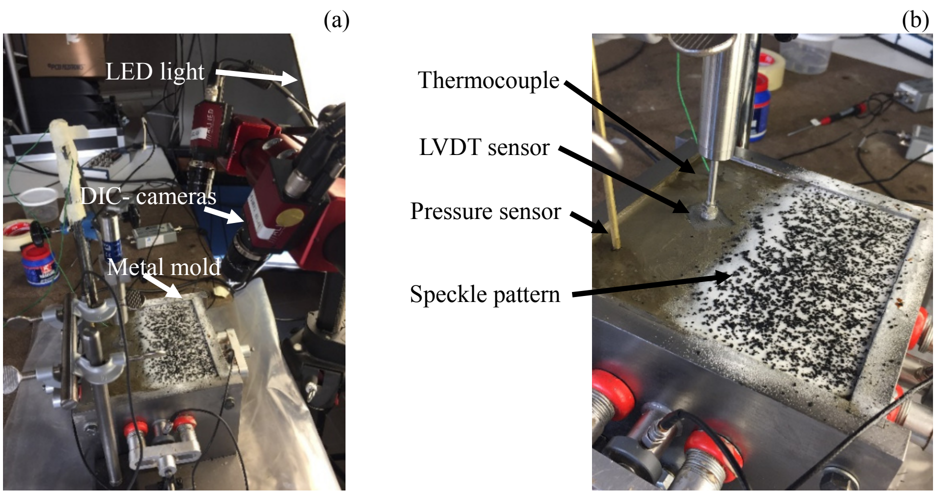

Fig. 1 (a) DIC system setup with metallic mould, (b) specimen surface covered with powder speckle pattern including thermocouple, LVDT and pressure sensors.

type was CNG 1.4/12-0902 with a focal length of 12 mm. The cameras were set at 200 mm from the specimen surface. White light was installed above the sample surface to provide lighting to the monitoring area during the measurement. On the specimen surface white-black speckle pattern was created as shown in **Fig. 1(b)**. Steel fine mesh is used to distribute the white aluminium oxide powder and black carbon powder on the specimen surface. Firstly, a layer of white aluminium oxide powder was applied through a sieve. Afterwards, in the same way well-distributed black dots of carbon powder are applied through a sieve on the surface to create a white/black speckle pattern. This means that the top layer is painted with randomly distributed black/ white pattern through a sieve to perform DIC measurements. Only the half of the sample surface is covered with speckle pattern since in the other half the vertical LVDT is placed. Therefore, DIC can visualize an area at which the left, right and bottom sides as shown in **Fig. 1(b)** are attached to the metallic mould and the top side stands in the middle area of the sample. The boundary conditions are not identical for all four sides of the analysis area. The total DIC field of view is 130 x 64 mm for cement paste and 150 x 75 mm for cement mortar. DIC analysis were performed with 61 x 61 subsets with a step size of 10 between subset centres (Gaussian subset weights, optimized 8-tap interpolation with normalized square differences). Images are captured every 120 s.

The measurement and the post-processing analysis were conducted using VIC-Snap software from Correlated Solutions, Inc. and 3D-digital image correlation tool (VIC-3D) provided by Correlated Solutions, Inc.

DIC monitoring started up to 20 min after casting. Reference starting point (Time 0) is considered the time of casting and the duration of the experiment was approximately 65 h. Furthermore, a linear variable differential transformer (LVDT) was installed vertically on the sample surface to measure the settlement. The vertically arranged LVDT tip touched a 20 x 20 mm metallic wire lattice that was applied on the specimen top surface, see **Fig. 1(b)**. As a result, the sensor tip was prevented from direct penetration into the viscous paste.

Besides the settlement, capillary pressure development of the specimen was monitored by a pressure sensor, see **Fig. 1(b)**. A pressure sensor was connected to a 150 mm long brass tube with an inside diameter of 4 mm. The brass tube was filled with de-ionized and outgassed water to allow monitoring the pressure development. The capillary pressure sensor was placed vertically 30 mm deep into the material from the top surface permitting the connection to the pore system.

In addition to the surface settlement and the capillary pressure, thermocouple was used simultaneously to measure the temperature development of the specimen indicating the progression of the hydration process as shown in **Fig. 1(b)**.

4. Results

4.1 Tracking settlement and understanding the hydration and drying mechanisms behind it

Figures 2(a) and **2(b)** illustrate the DIC average value of vertical displacement as measured considering the full-field surface for cement paste and cement mortar after casting, as average value for the whole monitored area (roughly accounting for half the specimen surface, as mentioned above). Settlement describes the vertical volume reduction caused by gravitational settlement of the solid particles in the fresh concrete (Combrinck *et al*. 2018). A large amount of surface settlement (vertical displacement) was recorded at very early age since the plastic material settles. Cement mortar achieves its maximum settlement with 1.3 mm/m after 150 min and beyond this moment mortar demonstrates a steady settlement evolution along the plastic state. The settlement increases at early stage for the cement paste while the curve presents fluctuations reaching its maximum value of 7.1 mm/m 1600 min after casting, see **Fig. 2(a)**. It is evident that the settlement development follows similar trends in both cases due to common cement material nature. However, the quantitative difference in settlement can be attributed to the materials composition, the addition of sand in the case of cement mortar and the different w/c ratios. **Fig. 2(b)** illustrates the DIC 3D surface settlement (vertical displacement) progression at different curing stages. It is noted that the settlement is

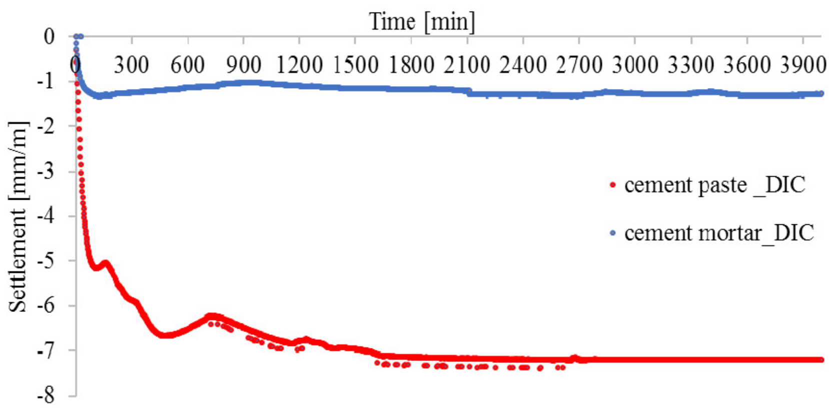

Fig. 2 (a) DIC vertical displacement (settlement) versus time for cement paste and cement mortar.

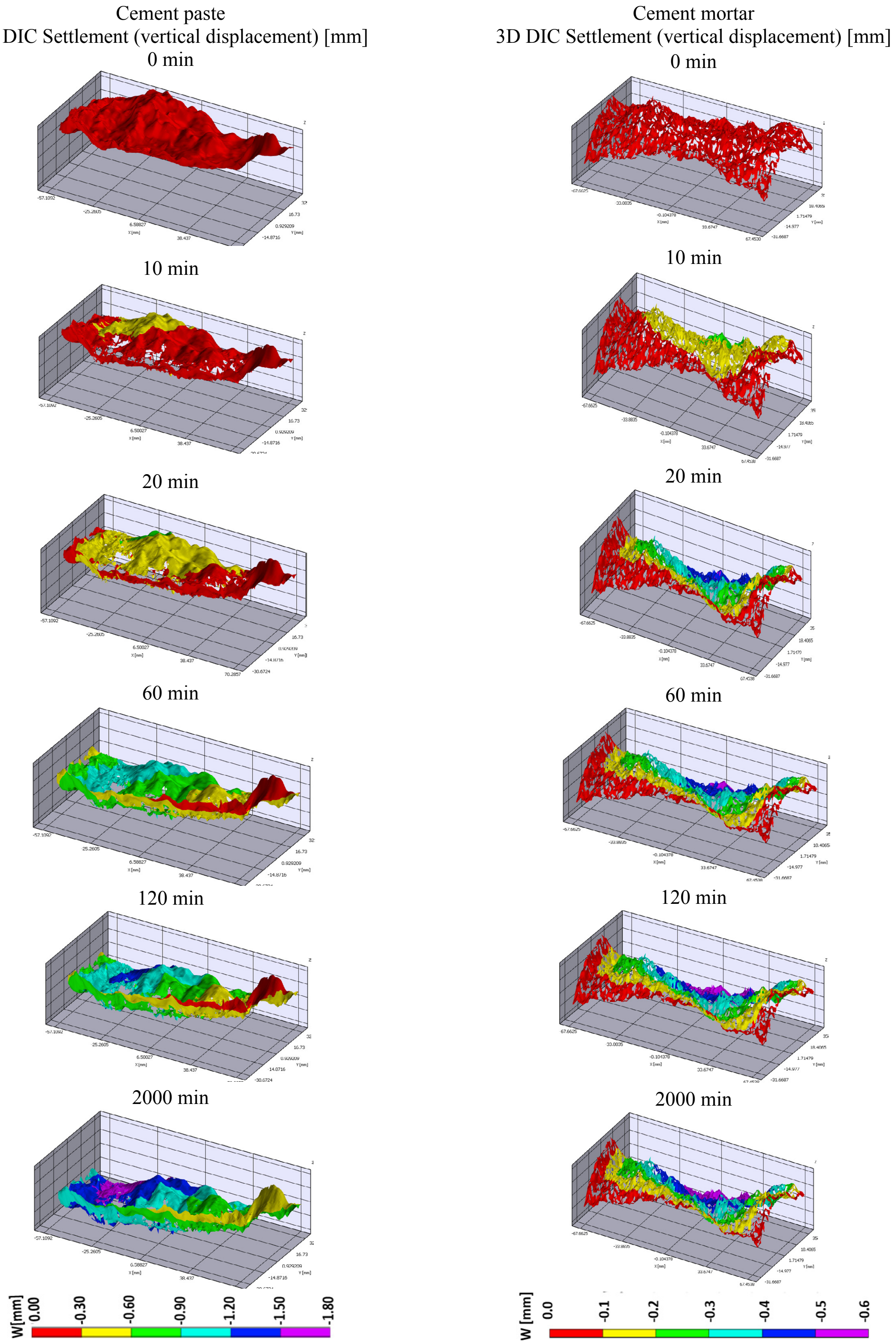

Fig. 2 (b) 3D DIC Settlement (vertical displacement) representatively shown for cement paste and cement mortar.

non-uniformly distributed at the surface.

The level of settlement can be related to the existence of the sand grains that offer volume stability in cement mortar. **Fig. 3** illustrates the temperature progress after casting for cement paste and mortar indicating the evolution of the hydration process. The temperature progress is monitored by applying thermocouples into the specimens.

During the first hours of drying, the specimen temperature drops due to the cement dissolution and initial hydration in the plastic state. It is interesting to note that the initial cement mortar temperature is 23°C while cement paste presents an initial temperature of 27°C. The temperature considerably increased after approximately 300 min from casting reaching 26°C for cement mortar and 44°C for cement paste representing the accelerated and dominant hydration process. It is demonstrated that the cement paste that carries higher cement content than the mortar reaches higher temperatures as hydration occurs. Since the hydration reaction occurs uniquely between the cement and the water, the addition of sand in the case of the mortar does not enhance the hydration process but does control the settlement evolution.

Both materials reach their peak approximately 740 min after casting indicating setting and strength onset. Beyond the temperature peak, both temperature curves drop progressively demonstrating the hardening progress and afterwards the temperature remains constant at low levels. It is interesting to note that the temperature peak coincides with a local peak of the settlement curves. This is attributed to the thermal expansion which reverses temporarily the settlement trend. This is more pronounced in the curve of paste, when between 600 and 900 min a relatively sharp peak is exhibited before the settlement curve becomes stable.

Furthermore, the drying process has a significant effect on the pore structure. The capillary pressure is additionally measured in an attempt to comprehensively track the curing process on cement-based media. After casting, a plane water film is formed at the material surface, known in literature as bleed water. As hydration begins, the bleed water diminishes as water evaporation accumulates. Consequently, the solid particles on material surface are no longer covered by bleed water and a pressure difference is built up between water and the surrounding air. Curved water surfaces (menisci) are now formed at the liquid phase between solid particles (Slowik *et al.* 2008). As hydration evolves, both capillary pressure and surface curvature progressively increase leading finally to contracting tensile forces between the particles since the water cannot longer bridge the pores and air penetrates the saturated pore system. The capillary pressure break-through is characterised by sudden drop of the capillary pressure (Slowik *et al.* 2014). The capillary pressure development and later drop is associated to drying process and can be indicative of plastic shrinkage, therefore tracking of it appears essential. In this study, pressure sensors were applied into the media and the pressure evolution is illustrated in **Fig. 4** for both cement mortar and cement paste.

The capillary pressure of cement paste increases after 150 min while cement mortar shows an increase immediately after casting. Cement paste presented a delayed increase of the capillary pressure indicating the increased bleed water at the surface. Indeed, the mass of water in the cement paste mixture was greater than the

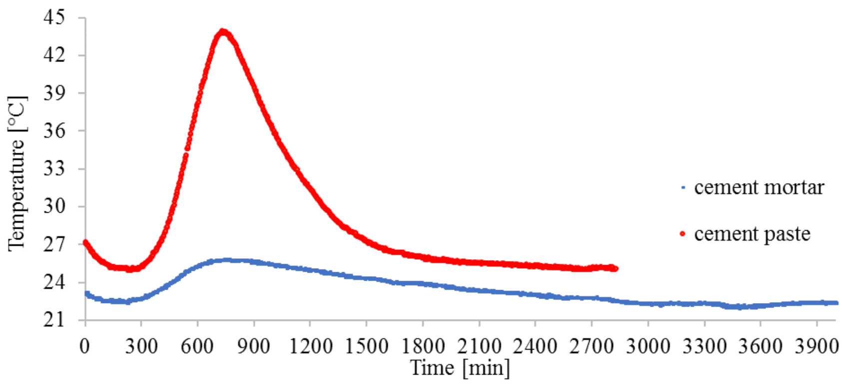

Fig. 3 Temperature evolution during curing for cement paste and cement mortar.

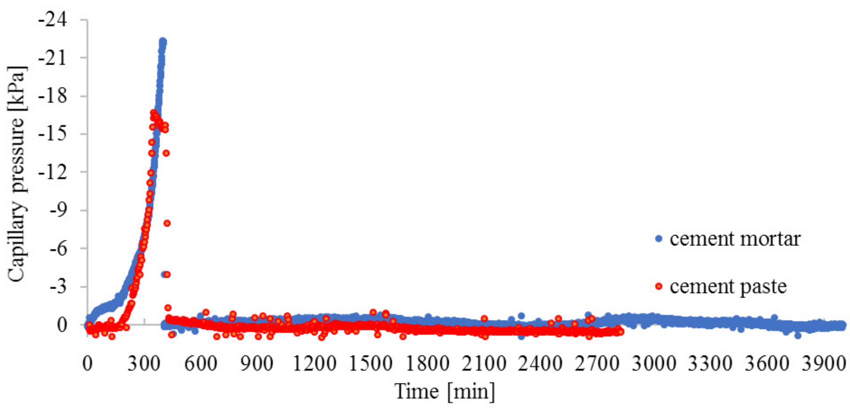

Fig. 4 Capillary pressure development in time for cement paste and cement mortar.

mortar one. This strong development of capillary pressure occurs simultaneously with the settlement progress in the plastic state as shown in **Fig. 2**. After 370 min the capillary pressure of cement paste drops with a negative peak value of -17 kPa. Cement mortar shows a negative peak value of -23 kPa and drops after 400 min. It is evident that cement paste characterised by higher water content is associated to delayed capillary pressure built up comparing to mortar. After the capillary pressure break-through the hydration process is accelerated as shown in temperature curves and the potential for plastic cracking achieve its maximum.

4.2 Full-field settlement assessment using DIC compared to conventional method

A fundamental difference between traditional sensing methods (i.e. LVDT point sensor) and DIC that should be highlighted is the fact that DIC measures the settlement in contactless mode, thereby the sensor cannot affect the measurement process, e.g., by increased settlement measured value due to self-weight of the sensor.

Apart from that, it is observed that LVDT point measurement of vertical displacement of a cementitious medium cannot be considered to fully assess surface settlement. The above statement is justified using DIC 3D full-field displacement maps illustrated in **Figs. 5(a)** and **5(b)** for both cement mortar and paste samples. It is proven that settlement of a point at the surface is influenced by its elevation compared to the surrounding areas (Dzaye *et al*. 2019). Settlement (in mm/m) is calculated as displacement W (in mm) divided by the nominal specimen depth (0.15 m) at points with the highest (P1), the lowest (P2) settlement, as an average considering the total average area. The DIC measurement are compared to classical LVDT point measurement.

Points P1 and P2 highlight the extreme cases of point measurement and LVDT and DIC average values stand in between. The P1-P2 settlement difference is measured at 8.1 mm/m and 3.3 mm/m for cement paste and mortar respectively. Additionally, the difference between the point LVDT and average DIC value is around 2 mm/m in both cases. The analysis demonstrates the limitation of unique point measurement of settlement, especially in the case of cement paste where the settlement range significantly varies.

The difference in settlement between LVDT and DIC measurement in the absolute value is attributed to the fact that DIC considers the total surface area and LVDT monitors the settlement at a point of the surface. It is evident that no robust conclusion can be obtained when considering only point analysis. This is an evidence for the significant enhancement offered by the global analysis. Using DIC the variation in settlement in different points is readily available while the average value on the surface can be regarded as a global measurement.

4.3 The effect of bleed water distribution on settlement

The settlement along a line that crosses the sample is illustrated in **Figs. 6(a)** and **6(b)** for cement paste and mortar in discrete monitoring stages in order to track the effect of bleed water and sample geometry on settlement distribution. In both cases the settlement has a non-homogeneous distribution along the sample with lower values obtained at the areas attached to mould walls. The settlement peak is detected at different locations: slightly to the left for the cement paste and in the middle zone in the case of mortar. The latter observation presents a randomness that may be related to the initial surface elevation map and the bleed water movement that influences the settlement progression. Different patterns were observed for all cases under study where the settlement peak was detected at different position each time. Apparently, the bleed water built up on material surface at the first minutes after casting fully controls the settlement distribution, phenomenon observed regardless the material composition (w/c, use of sand, etc.).

The effect of boundaries on settlement distribution is illustrated in **Fig. 7** where the settlement of cement mortar obtained 2320 min after casting is measured for three lines crossing the sample: L0 stands at the middle of the

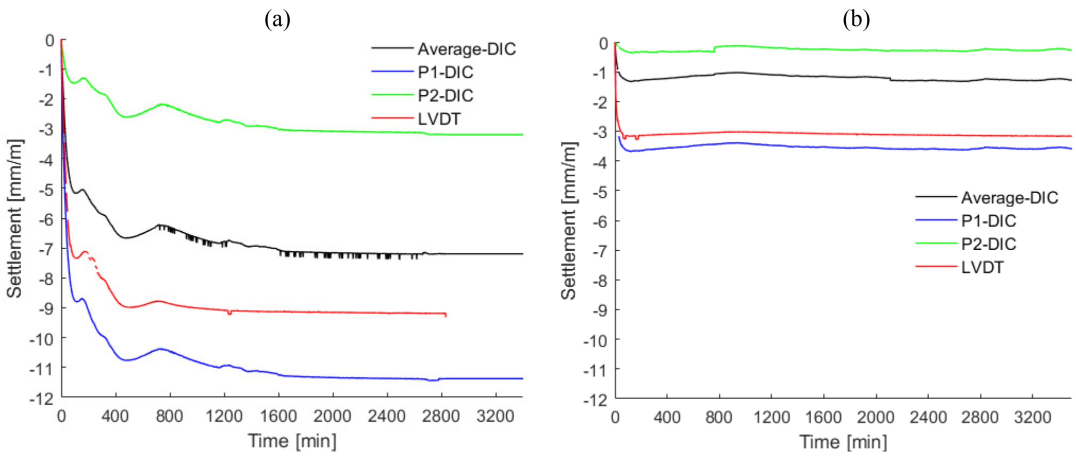

Fig. 5 Surface settlement of DIC (representatively P1, P2 and Average total area) and LVDT for (a) cement paste and (b) cement mortar sample.

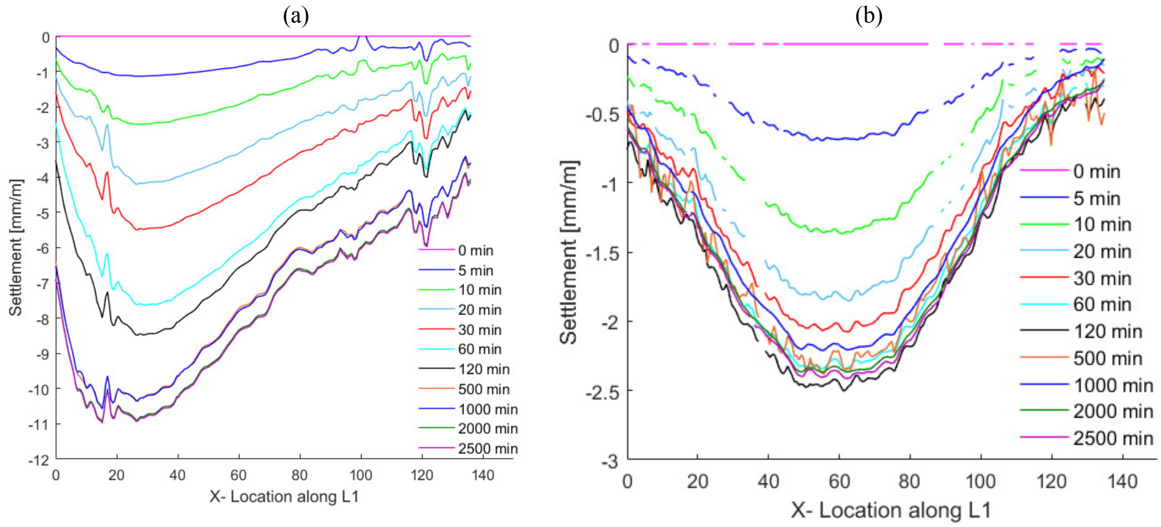

Fig. 6 DIC surface settlement along line L1 at discrete monitoring stages (a) cement paste and (b) cement mortar.

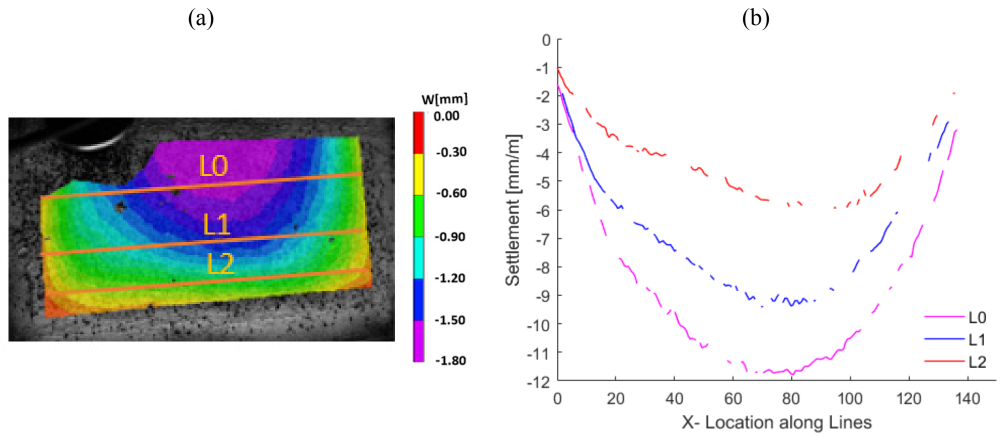

Fig. 7 (a) DIC Line analyses at different locations for cement mortar; (b) DIC surface settlement along lines (L0, L1 and L2).

sample, L1 further to the edges and L2 stands the closest to the edge. All three lines (L0, L1 and L2) illustrate similar trends but with different absolute values, thereby indicating the impact of the surface elevation close to the edge as well as the bleed water movement on the settlement progression. Line L0 is closer to the specimen centre and indicates the highest settlement while L2 is close to the edges indicating the lowest settlement. These results are consistent indicating the maximum settlement near the specimen centre for cement mortar.

5. Conclusions

This paper focuses on an effective and innovative technique of DIC to evaluate the settlement distribution of cement paste and cement mortar in fresh state (few minutes after casting) in a contactless mode. 3D-DIC allows monitoring the non-uniform settlement distribution at different locations on specimen surface by creating a powder speckle pattern. This approach realizes a deeper understanding of concrete consolidating process and expands the measurement data to the whole surface. The results clearly show the higher settlement of the paste compared to mortar, while they are sensitive enough to the hydration temperature peak that causes a transient expansion. In addition, the full-field character of the measurement confirms the differential settlement on the surface, something not possible with the classical LVDT point measurement. Further study should be done regarding the accuracy of the speckle pattern that is affected by the bleed water in the first hours after casting and the possible influence of aluminium oxide/carbon powder speckle pattern on the hydration process.

Acknowledgements

Financial support of the Research Foundation Flanders (FWO-Vlaanderen) through Projects No 28976 and G012315N is gratefully acknowledged.

References

Amziane, S., (2006). "Setting time determination of cementitious materials based on measurements of the hydraulic pressure variations." *Cement and Concrete Research,* 36(2), 295-304.

Barcelo, L., Boivin, S., Acker, P., Toupin, J. and Clavaud, B., (2011). "Early age shrinkage of concrete back to physical mechanisms." *Concrete Science and Engineering,* 3(10), 85-91.

Barranger, Y., Doumalin, P., Dupré, J. C. and Germaneau, A., (2010). "Digital image correlation accuracy: Influence of kind of speckle and recording setup." *EPJ Web of Conferences,* 31002.

Bertil, P. and Göran, F., (2002). "*Self-desiccation and its importance in concrete technology*." Division o. Lund: proceedings of the third international research seminar in Lund.

Carlson, J., Nilsson, M., Fernández, E. and Planell, J. A., (2003). "An ultrasonic pulse-echo technique for monitoring the setting of $CaSO_4$-based bone cement." *Biomaterials,* 24(1), 71-77.

Cohen, M. D., Olek, J. and Dolch, W. L., (1990). "Mechanism of plastic shrinkage cracking in portland cement and portland cement-silica fume paste and mortar." *Cement and Concrete Research*, 20(1), 103-119.

Combrinck, R., Steyl, L. and Boshoff, W. P., (2018). "Interaction between settlement and shrinkage cracking in plastic concrete." *Construction and Building Materials*, 185, 1-11.

Dzaye, E. D., De Schutter, G. and Aggelis, D., (2018a). "Application of digital image correlation to cement paste." In: *Proceeding of 18th International Conference on Experimental Mechanics (ICEM 2018)*, Brussels, Belgium, July 1-5, 2018, 2-7.

Dzaye, E. D., De Schutter, G. and Aggelis, G., (2018b). "Monitoring fresh cementitious material by digital image correlation (DIC)." In: *Proceedings of SynerCrete18*, Funcal, Portugal. 24-26 October, RILEM, 267-272.

Dzaye, E. D., Tsangouri, E., Spiessens, K., De Schutter, G. and Aggelis, D. G., (2019). "Digital image correlation (DIC) on fresh cement mortar to quantify settlement and shrinkage." *Archives of Civil and Mechanical Engineering,* 19(1), 205-214.

Geike, M. and Knudsen, T., (1982). "Chemical shrinkage of Portland cement paste." *Cement and Concrete Research*, 12(5), 603-610.

Kurdowski, W., (2014). "*Cement and concrete chemistry*." 1st ed. Krakow, Springer.

Kwak, H.-G., Ha, S., Weiss, W. J. and Asce, M., (2010). "Experimental and numerical quantification of plastic settlement in fresh cementitious systems." *Journal of Materials in Civil Engineering*, 22(10), 951-966.

Lagier, F., Jourdain, X., De Sa, C., Benboudjema, F. and Colliat, J. B., (2011). "Numerical strategies for prediction of drying cracks in heterogeneous materials: Comparison upon experimental results." *Engineering Structures,* 33(3), 920-931.

Lecompte, D., Smits, A., Bossuyt, S., Sol, H., Vantomme, J., Van Hemelrijck, D. and Habraken, A. M., (2006). "Quality assessment of speckle patterns for digital image correlation." *Optics and Lasers in Engineering,* 44(11), 1132-1145.

Lionello, G., Sirieix, C. and Baleani, M., (2014). "An effective procedure to create a speckle pattern on biological soft tissue for digital image correlation measurements." *Journal of the Mechanical Behavior of Biomedical Materials*, 39, 1-8.

Lura, P., Mazzotta, G. B., Rajabipour, F. and Weiss, J., (2006). "Evaporation, settlement, temperature evolution, and development of plastic shrinkage cracks in mortars with shrinkage-reducing admixtures." In: *Proceedings of RILEM-JCI Seminar on Concrete Durability and Service Life Planning (ConcreteLife'06)*, 1, 1-11.

Maruyama, I. and Sasano, H., (2013). "Strain and crack distribution in concrete during drying." *Materials and Structures*, 47(3), 517-532. no. 546.

Mauroux, T., Benboudjema, F., Turcry, P., Aït-mokhtar, A. and Deves, O., (2012). "Study of cracking due to drying in coating mortars by digital image correlation." *Cement and Concrete Research,* 42(7). 1014-1023.

Pease, B., Hossain, A. B. and Weiss. J., (2004). "Quantifying volume change, stress development, and cracking due to early-age autogenous shrinkage." *Aci Special Publications*, 220, 23-38.

Sant, G., Dehadrai, M., Lura, P., Bentz, D., Ferraris, C. F., Bullard, J. W. and Weiss, J., (2009). "Detecting the fluid-to-solid transition in cement pastes: part II---Comparison of experimental and numerical techniques." *Concr. Intl.*, June, 53-58.

Slowik, V., Schmidt, M. and Fritzsch, R., (2008). "Capillary pressure in fresh cement-based materials and identification of the air entry value." *Cement and Concrete Composites*, 30(7), 557-565.

Slowik, V., Schmidt, M., Kässler, D. and Eiserbeck, M., (2014). "Capillary pressure monitoring in plastic concrete for controlling early-age shrinkage cracking." *Transportation Research Record: Journal of the Transportation Research Board*, 2441(1), 1-5.

Sutton, M. A., Orteu, J. J. and Schreier, H. W., (2009). "*Image correlation for shape, motion and deformation measurements, basic concepts, theory and applications*." New York, Springer.

Taylor, P. C., Johansen, V. C., Graf, L. A., Kozikowski, R. L., Zemajtis, J. Z. and Ferraris, C. F., (2006). "*Identifying incompatible combinations of concrete materials*: *- Volume II – Test protocol*" U.S. Department of Transportation Federal Highway Administration, Technical Report, HR T-06-080.

Topu, I. B., Uygunolu, T. and Hocaolu, I., (2012). "Electrical conductivity of setting cement paste with different mineral admixtures." *Construction and Building Materials* 28 (1): 414-420.

Weyers, R. E., Conway, J. C. and Cady, P. D., (1982). "Photoelastic analysis of rigid inclusions in fresh concrete." *Cement and Concrete Research,* 12(4), 475-484.

Wierig, H. J. (Ed.), (1990). "*Properties of fresh concrete*." Proceedings of the RILEM Colloquium. Hanover, CRC Rress, 400.

Wittmann, F. H., (1976). "On the action of capillary pressure in fresh concrete." *Cement and Concrete Research*, 6(1), 49-56.

Yamakawa, M., Hashimoto, C., Watanabe, T. and Yokote, S., (2003). "Study on settlement crack for reinforced concrete structures using the concrete with type IV fly ash." *International Journal of Modern Physics,* 17, 1470-1475.